Supporting figures for

‘**Molecular recognition of human ephrinB2 cell surface receptor by an emergent African henipavirus**’

This file includes: Supplementary Figures S1-S9, Supplementary Table S1, and Supplementary References.

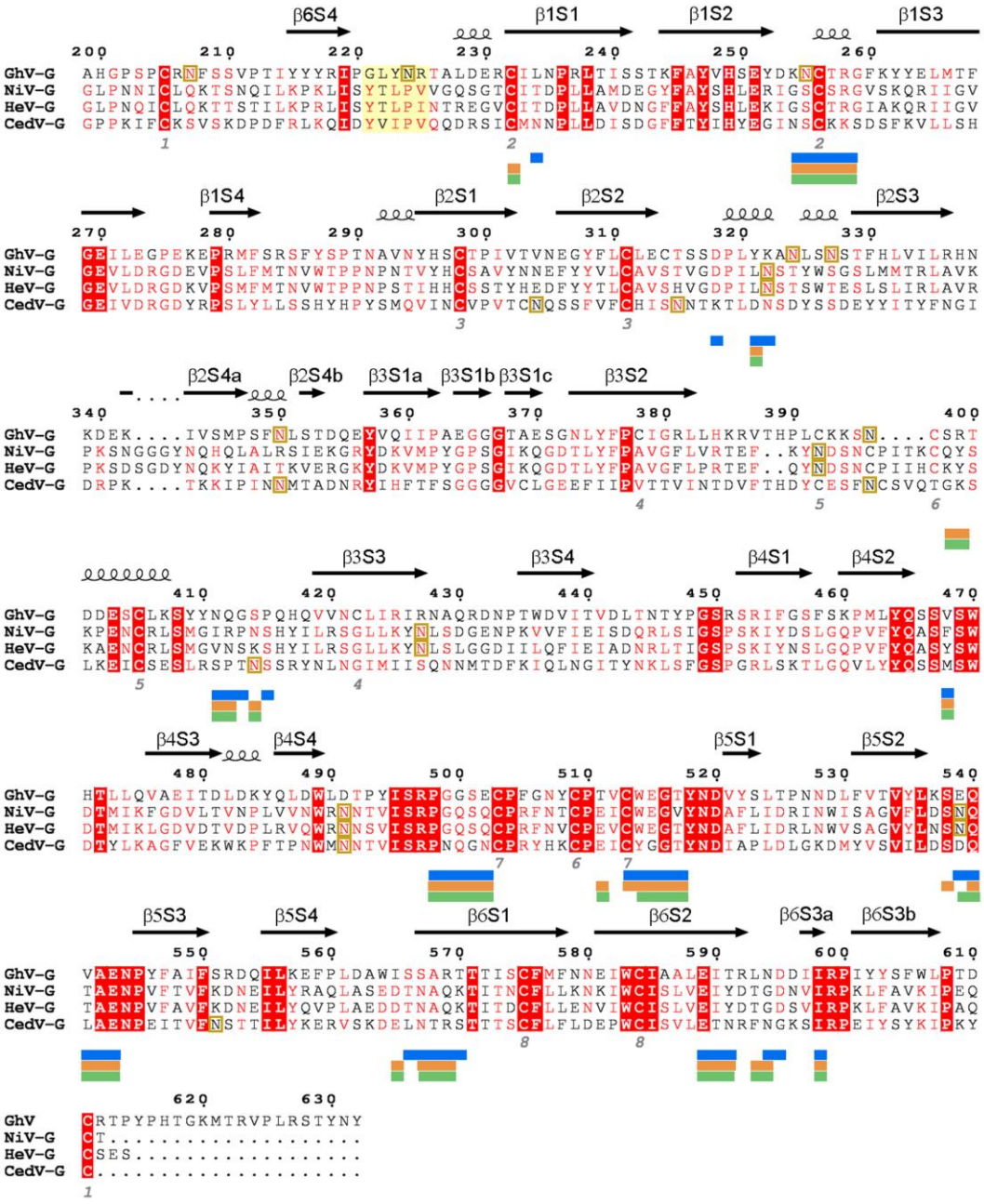

Fig. S1. Structure-based sequence alignment of the globular β-propeller domain of GhV-G with NiV-G, HeV-G and CedV-G (determined by Multalin (1) and plotted with ESPript 3 (2)). Secondary structure elements are shown with an arrow (β-strand) and spiral (α-helix) and are labelled according to standard paramyxovirus nomenclature. Residues highlighted red are fully conserved, residues which are colored red are partially conserved, and residues which are black are not conserved. *N*-linked glycosylation sites are indicated by yellow rectangles. Residues of

GhV-G, NiV-G, and HeV-G glycoproteins occluded in the ephrinB2 interface are indicated by blue, orange, and green lines, respectively (as determined with the PDBePISA server, http://www.ebi.ac.uk/pdbe/pisa/ (3)). Disulphide bond pairs are indicated with grey numbers below the sequence. Residues in the shaded yellow box between β6S4 and β1S1 are critical for the Mab45 receptor-binding epitope (see "Determinants of receptor-mediated fusion" relating to Fig. 7 in the results section of the main text)(4).

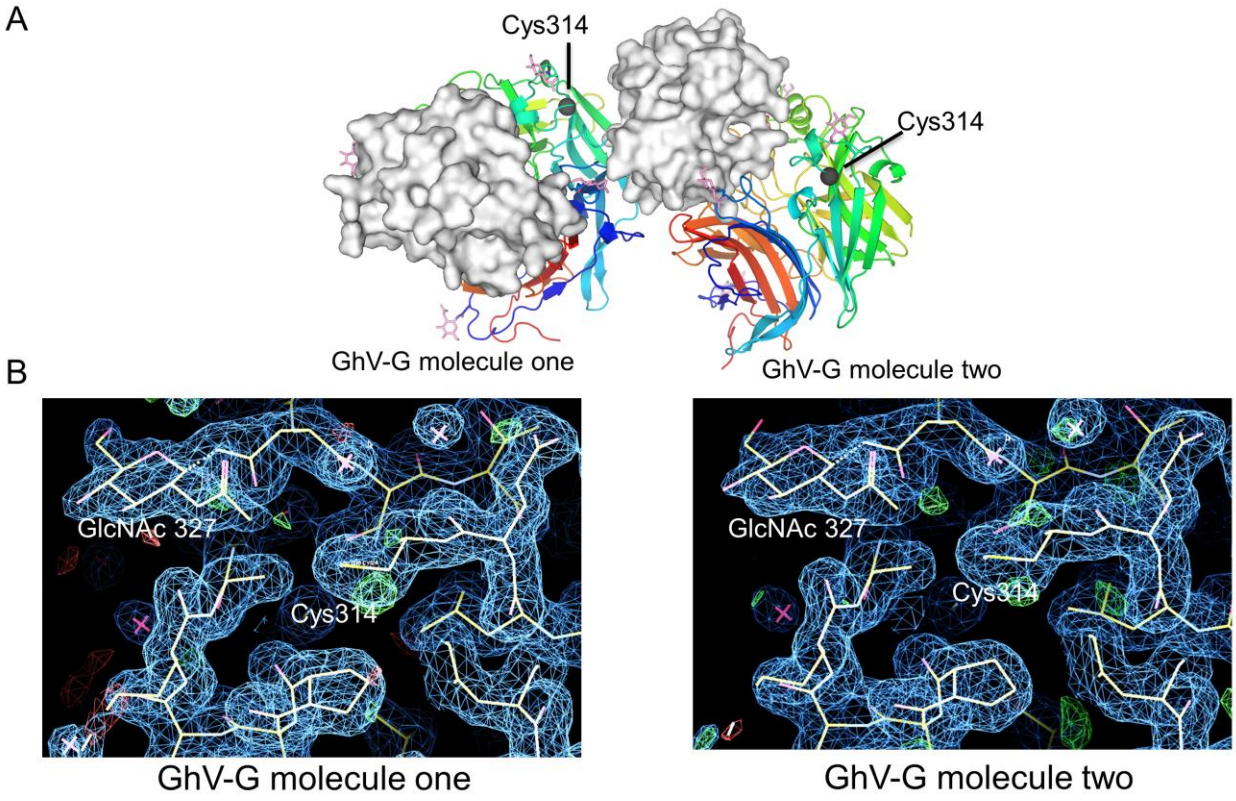

Fig. S2. The unpaired cysteine of GhV-G. (A) The two complexes of GhV-G-ephrinB2 observed in the asymmetric unit. Each GhV-G protomer of the dimer is shown with cartoon representation and colored as a rainbow with the N-terminus shown in blue and the C-terminus red. EphrinB2 is shown as a white surface. Carbohydrate moieties (GlcNAc) observed at N-linked glycosylation sites are shown as pink sticks. Residues corresponding to Cys314 are colored as black spheres. (B) The free cysteine '314' is buried under glycan Asn327 with some solvent accessibility. A maximum likelihood-weighted 2*Fo-Fc* electron density map is shown around Cys314 from the two GhV-G molecules observed in the asymmetric unit.

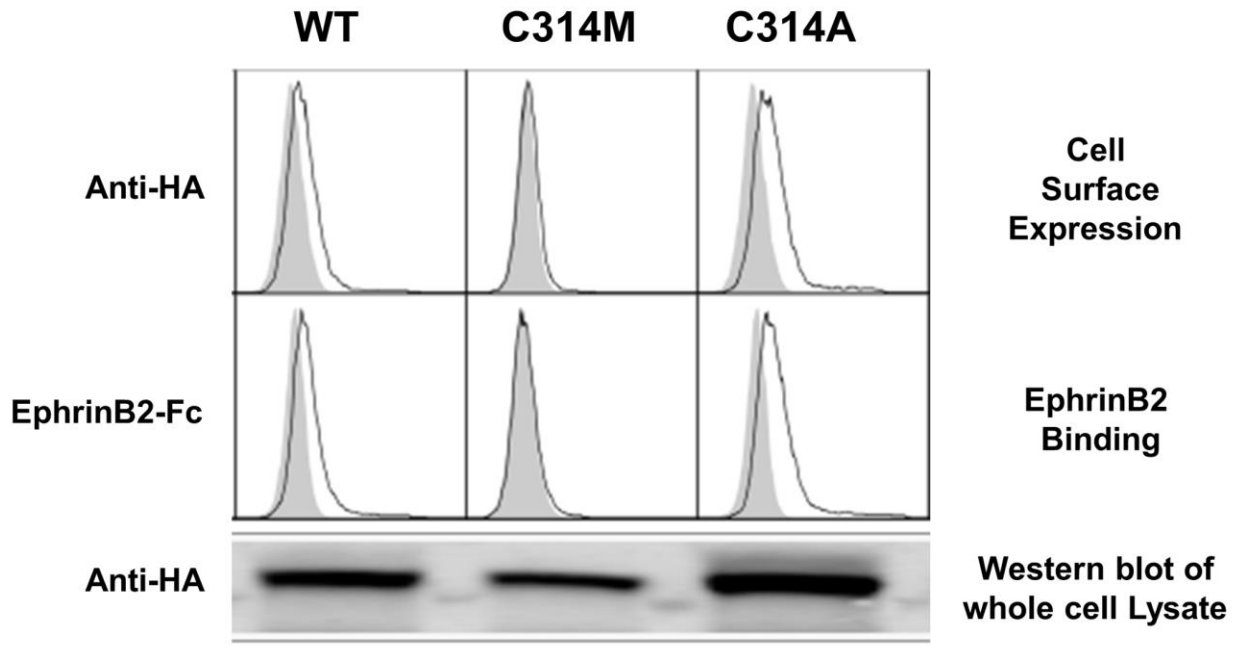

Fig. S3. C-terminally HA-tagged wild-type GhV-G or the indicated C314 mutants were transiently transfected into CHO cells. 24 hours post-infection, cell surface expression and ephrinB2 binding were determined by anti-HA and EphrinB2-Fc staining, respectively. Transfected CHO cells in duplicate wells were lysed and whole cell lysates were western-blotted with anti-HA antibodies.

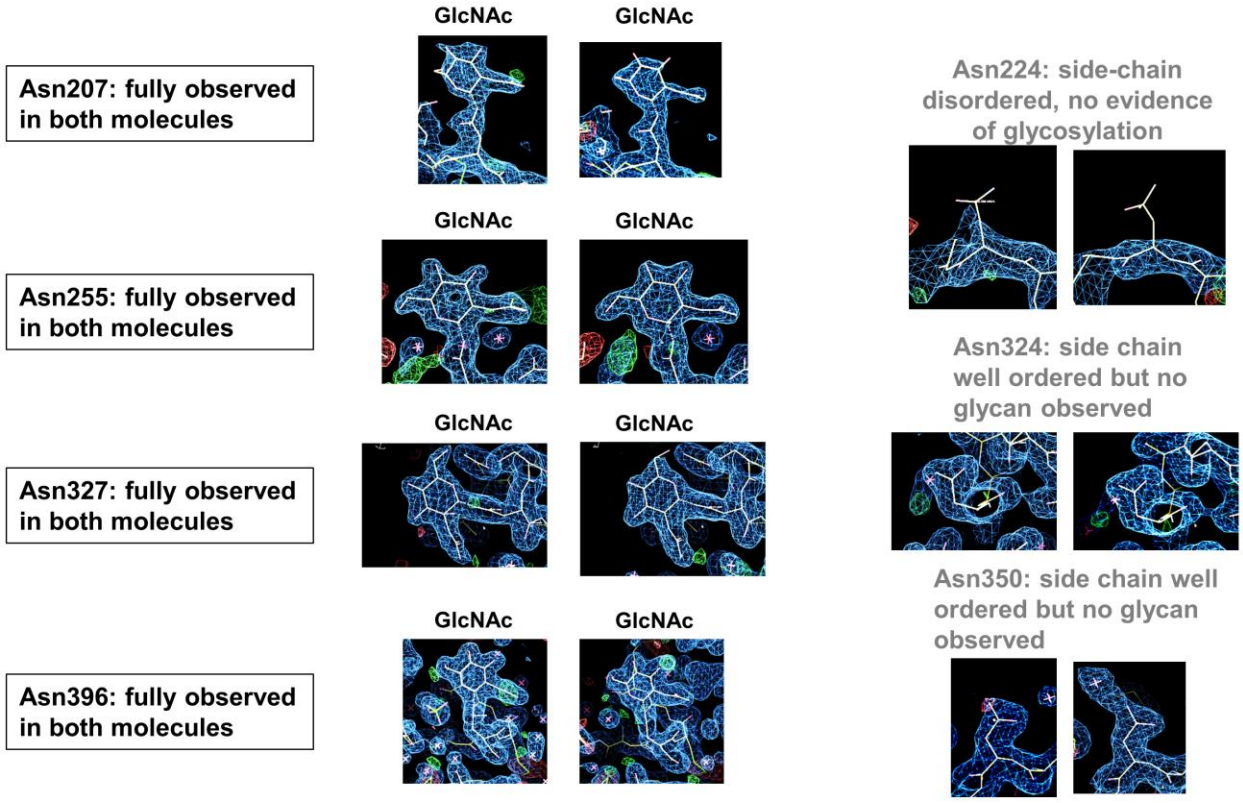

Fig. S4. Electron density at N-linked glycosylation sequons. Maximum likelihood-weighted 2*Fo-Fc* electron density is shown around each N-linked glycosylation sequon. Well-ordered *N*-acetylglucosamine (GlcNAc) residues were observed at Asn207, Asn255, Asn327, and Asn396. However, no electron density for these moieties was observed at Asn224, Asn324, and Asn350, suggesting that either these N-linked glycan sites are either not occupied or that the GlcNAc residues were too flexible to be observed in the crystal.

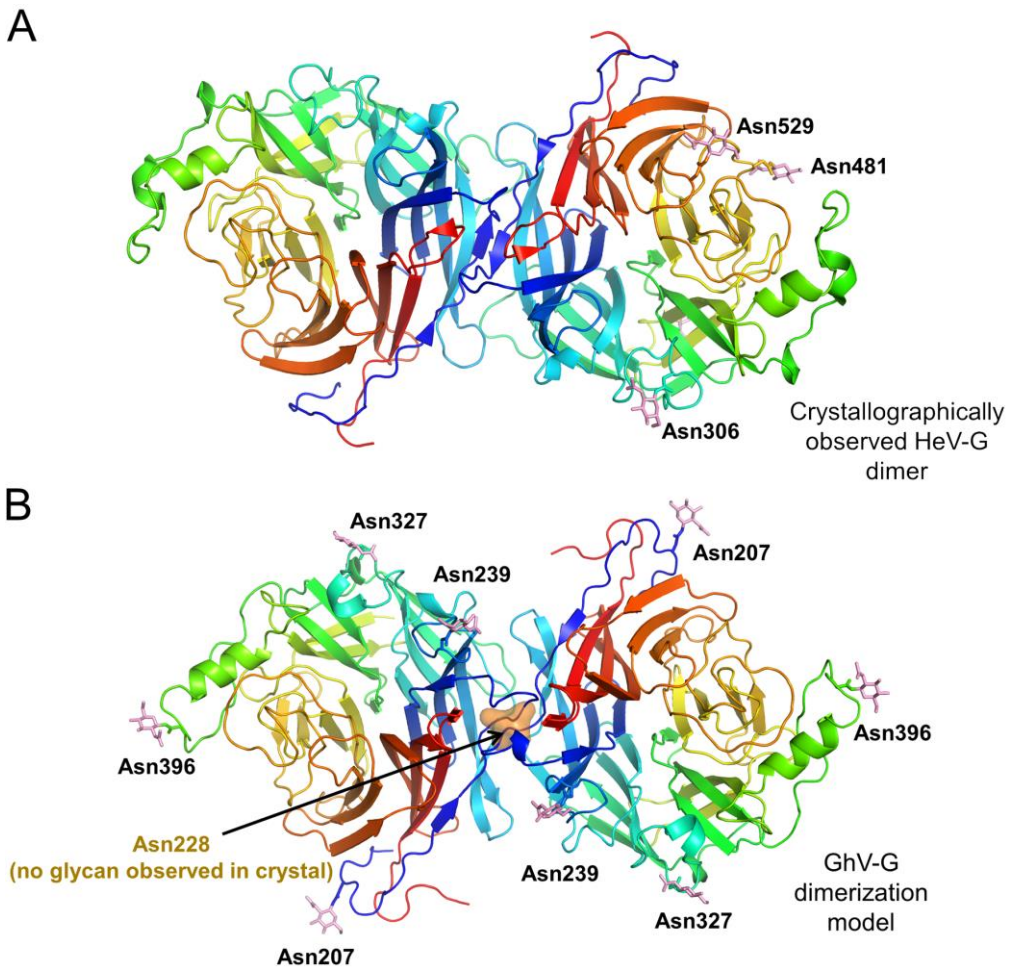

Fig. S5. Analysis of whether GhV-G is likely to oligomerize as observed in the crystal of HeV-G. (A) Crystal structure analysis of HeV-G receptor binding domain (PDB ID 2X9M (5)) revealed a dimeric conformation similar to that commonly observed in crystal structures of other paramyxovirus attachment glycoproteins (6-10). The HeV-G dimer is shown in cartoon representation with observed N-linked glycosylation sites shown as pink sticks. Each protomer of the dimer is colored as a rainbow with the N-terminus blue and the C-terminus red. (B) A GhV-G dimerization model, based upon superposition of GhV-G onto both protomers of the HeV-G dimer (n.b. there was no evidence of dimerization in the GhV-G-ephrinB2 structure or in the crystallographic packing). The position of the putative N-linked glycosylation sequon at Asn228 would likely impede GhV-G glycoprotein dimerization. This suggests that either Asn228 is not glycosylated, the loop of residues 218-228 are in a different conformation than in NiV-G or HeV-G, or that GhV-G oligomerizes differently than other paramyxoviruses.

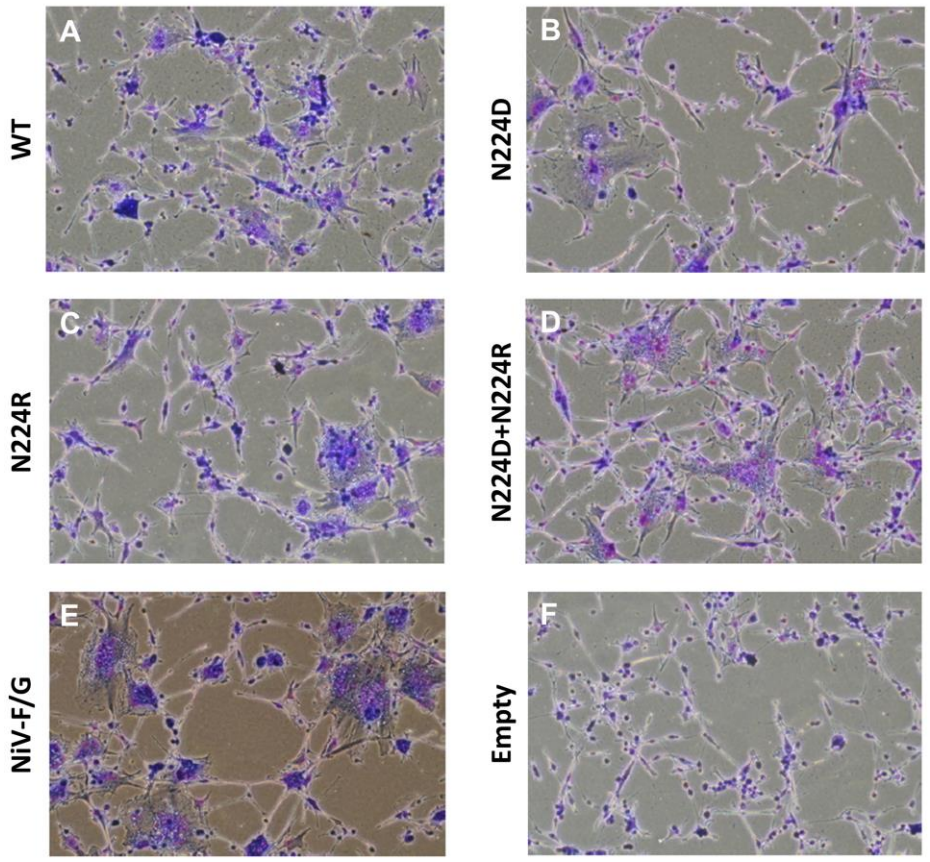

Fig. S6. Mutation of potential N-linked glycosylation site at putative dimer interface has no effect on GhV-G mediated fusion. A syncytia formation assay in transfected U87 glioblastoma cells was performed as described in methods. Briefly, a 1:1 ratio of codon-optimized expression plasmids for wt GhV-F, GhV-G (or the indicated N223 mutants) were transfected into U87 cells plated in 12-wells, and syncytia formation was observed 12-16 hours post-transection after Giemsa staining to visulaize syncytia. U87 cells endogenously express high levels of ephrinB2 and are highly permissive for HNV envelope-mediated syncytia formation (11). (A) Wt NiV-G, (B) N223D, (C) N223R, (D) N223D + N223R (a 1:1 mixture of both mutants to give the same total amount of GhV-G transfected), (E) Wt NiV-F/G (positive control) and (F) empty vector (negative control). Nuclei per syncytium were counted from at least five random fields using Image J software where a syncytium was defined as four or more nuclei sharing the same cytoplasm. The average of number per syncytium was ~24 (range 8 -75) for the NiV-F/G positive control. No syncytia were observed in the empty vector transfected cells. Although GhV-F/G formed fewer and smaller syncytia than NiV-F/G (average ~10), neither the N223D nor the N223R mutant showed any obvious deficiencies when compared wild-type GhV-G.

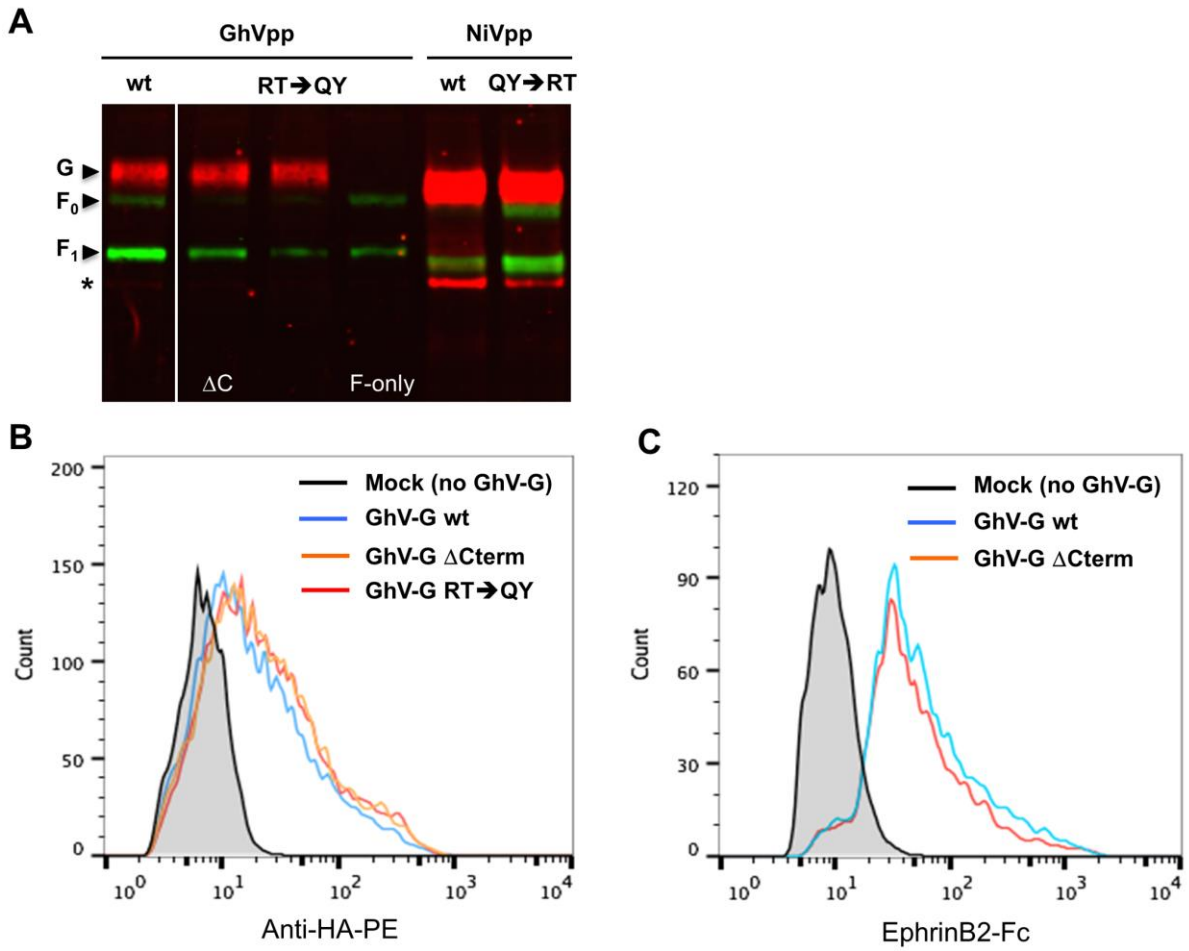

Fig. S7. Envelope glycoprotein expression on the GhV and NiV pseudotyped particles used for virus entry assays. (A) Purified GhVpp and NiVpp were immunoblotted for F and G expression as described in the Methods. GhV-F and G migrates slightly higher than NiV-F and G, as expected from their predicted molecular mass. The asterisk marks for a likely break-down product of G, it is seen in most lanes except for the negative control lane that does not contain any G (F-only). Delta C refers to the nine amino acid C-terminal truncation that is investigated later in Fig. 7 of the main text. It is shown here for convenience of comparisons. GhV-G is incorporated into pseudotyped particles at lower levels than NiV-G, consistent with the relative lower expression of GhV-G shown in Fig. 1. However, wild-type HNV-Gs and their respective mutants are incorporated at the same levels. (B) Cell surface expression of GhV-G and the various mutants examined in this study. HA-staining was used to verify cell surface expression as all constructs were HA-tagged at their extracellular C-terminus. (C) Soluble EphrinB2-Fc staining of GhV-G wt and GhV-G delta C-term expressed on transiently transfected CHO cells.

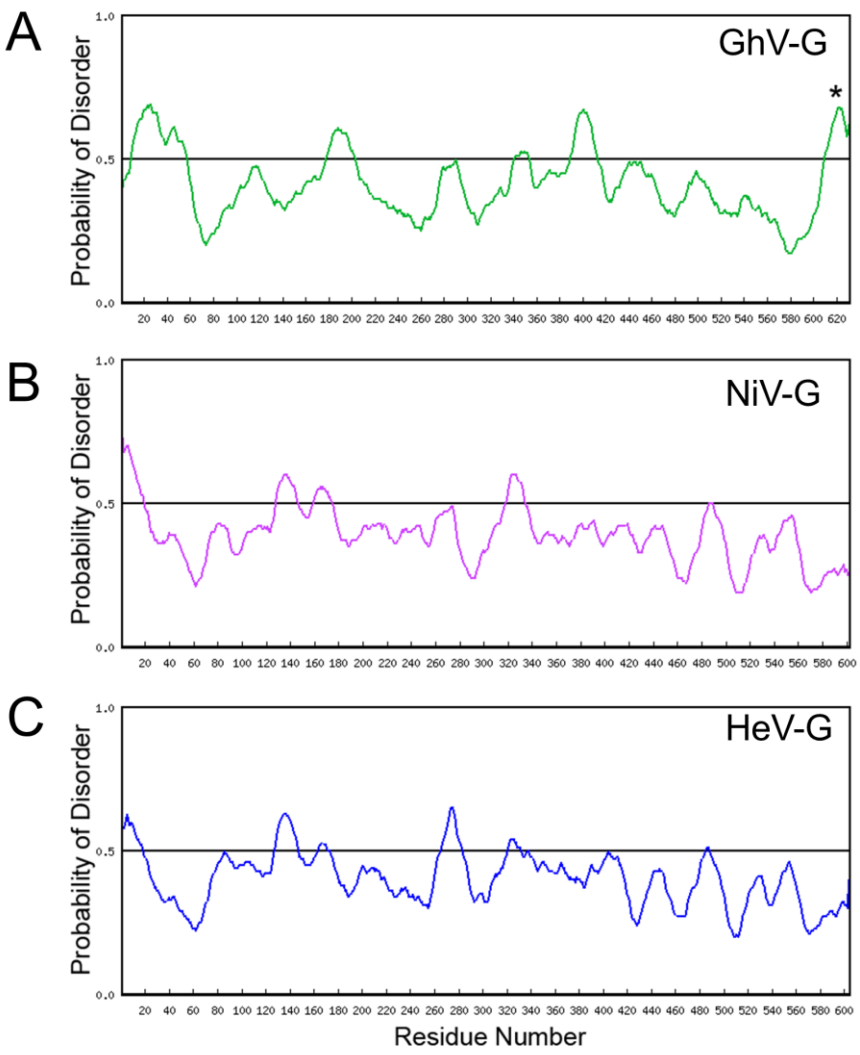

Fig. S8. Structure disorder prediction analysis performed with RONN (https://www.strubi.ox.ac.uk/RONN) for the attachment glycoproteins from (A) GhV, (B) NiV, and (C) HeV. The asterisk in panel (A) denotes the seventeen amino acid C-terminal extension, which is only observed in GhV-G and has high likelihood of being disordered.

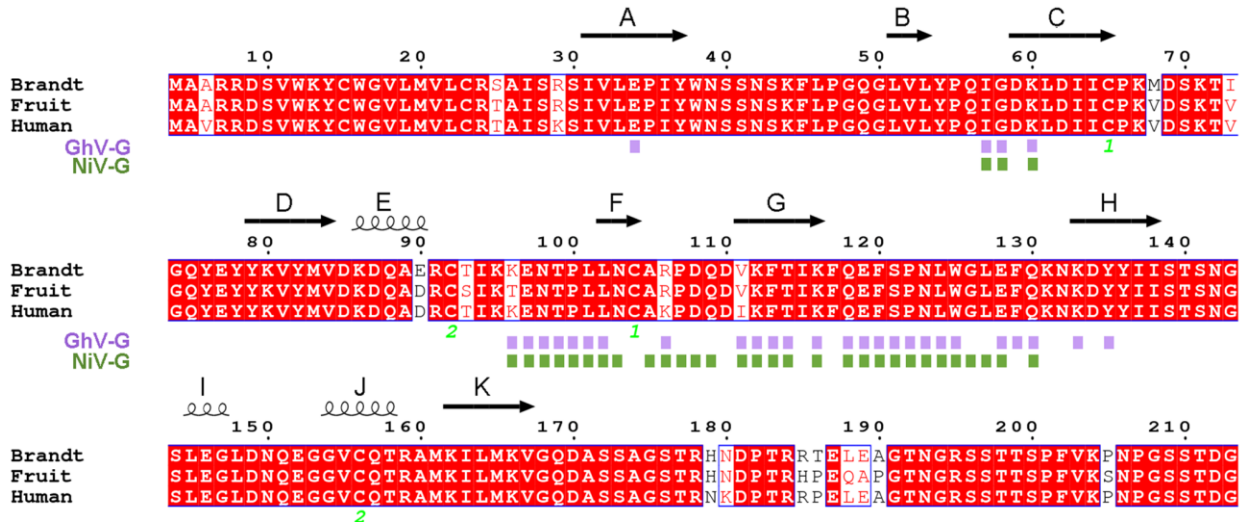

Fig. S9. Structure-based sequence alignment of human and bat ephrinB2 sequences (determined by Multalin (1) and plotted with ESPript 3 (2)). Human (GenBank accession number NP_004084.1), Brandt's bat (GenBank accession number XP_005884537.1) and fruit bat (GenBank accession number NP_001277099.1) sequences are shown. Secondary structure elements are shown with an arrow (β-strand) and helix (α-helix) and are labelled according to standard ephrin nomenclature. Disulphide bonds pairs are numbered below the sequences in green. Residues occluded in GhV-G-ephrinB2 and NiV-G-ephrinB2 interfaces (as determined with the PDBePISA server, http://www.ebi.ac.uk/pdbe/pisa/) are labeled with purple and green boxes, respectively. Fully conserved residues are highlighted red, partially conserved residues are colored red, and residues colored black are not conserved.

Table S1. **Summary of HNV-G-ephrinB2 crystal structures.**

	GhV-G	NiV-G	HeV-G
Interface area (Å^2)[1,2]	~2,400	~2,800	~2,700
Overlay of six-bladed β-propeller	1.7 Å r.m.s.d. (GhV-G vs NiV-G)	0.8 Å r.m.s.d. (NiV-G vs HeV-G)	
No. disulfide bonds (S-S)[3]	8	7	7
No. cysteines in the β-propeller domain	17 (C314 is unpaired)	14	14
PNGS[4] in the receptor-binding-domain	4/7	5/5	5/5
Residues after C-terminal cysteine	21	1	3

[1]Surface area calculated with PISA server (http://www.ebi.ac.uk/pdbe/pisa/).
[2]Average EphB–ephrinB2 interface area is ~1,500 Å^2.
[3]Two to five disulfide bonds are observed for attachment glycoproteins (HN/H) from other *Paramyxovirinae* genera.
[4]PNGS, putative N-linked glycosylation site.

Supplementary References

1. Corpet F (1988) Multiple sequence alignment with hierarchical clustering. *Nucleic Acids Res.* 16(22):10881-10890.
2. Robert X & Gouet P (2014) Deciphering key features in protein structures with the new ENDscript server. *Nucleic acids research* 42(Web Server issue):W320-324.
3. Krissinel E & Henrick K (2007) Inference of macromolecular assemblies from crystalline state. *J. Mol. Biol.* 372(3):774-797.
4. Aguilar HC*, et al.* (2009) A novel receptor-induced activation site in the Nipah virus attachment glycoprotein (G) involved in triggering the fusion glycoprotein (F). *J. Biol. Chem.* 284(3):1628-1635.
5. Bowden TA, Crispin M, Harvey DJ, Jones EY, & Stuart DI (2010) Dimeric architecture of the Hendra virus attachment glycoprotein: evidence for a conserved mode of assembly. *J. Virol.* 84(12):6208-6217.
6. Welch BD*, et al.* (2013) Structure of the parainfluenza virus 5 (PIV5) hemagglutinin-neuraminidase (HN) ectodomain. *PLoS pathogens* 9(8):e1003534.
7. Yuan P*, et al.* (2011) Structure of the Newcastle disease virus hemagglutinin-neuraminidase (HN) ectodomain reveals a four-helix bundle stalk. *Proceedings of the National Academy of Sciences of the United States of America* 108(36):14920-14925.
8. Crennell S, Takimoto T, Portner A, & Taylor G (2000) Crystal structure of the multifunctional paramyxovirus hemagglutinin-neuraminidase. *Nat. Struct. Biol.* 7(11):1068-1074.
9. Lawrence MC*, et al.* (2004) Structure of the haemagglutinin-neuraminidase from human parainfluenza virus type III. *J. Mol. Biol.* 335(5):1343-1357.
10. Yuan P*, et al.* (2005) Structural studies of the parainfluenza virus 5 hemagglutinin-neuraminidase tetramer in complex with its receptor, sialyllactose. *Structure* 13(5):803-815.
11. Pernet O*, et al.* (2014) Evidence for henipavirus spillover into human populations in Africa. *Nature communications* 5:5342.